

UC San Diego

UC San Diego Previously Published Works

Title

Bimodal activation of BubR1 by Bub3 sustains mitotic checkpoint signaling

Permalink

<https://escholarship.org/uc/item/9xh2p1w3>

Journal

Proceedings of the National Academy of Sciences of the United States of America,
111(40)

ISSN

0027-8424

Authors

Han, Joo Seok
Vitre, Benjamin
Fachinetti, Daniele
et al.

Publication Date

2014-10-07

DOI

10.1073/pnas.1416277111

Peer reviewed

Bimodal activation of BubR1 by Bub3 sustains mitotic checkpoint signaling

Joo Seok Han^{a,b,1}, Benjamin Vitre^{a,b,2}, Daniele Fachinetti^{a,b,2}, and Don W. Cleveland^{a,b,c,1}

^aLudwig Institute for Cancer Research and Departments of ^bCellular and Molecular Medicine and ^cMedicine, University of California, San Diego, La Jolla, CA 92093

Contributed by Don W. Cleveland, August 25, 2014 (sent for review May 6, 2014)

The mitotic checkpoint (also known as the spindle assembly checkpoint) prevents premature anaphase onset through generation of an inhibitor of the E3 ubiquitin ligase APC/C, whose ubiquitination of cyclin B and securin targets them for degradation. Combining in vitro reconstitution and cell-based assays, we now identify dual mechanisms through which Bub3 promotes mitotic checkpoint signaling. Bub3 enhances signaling at unattached kinetochores not only by facilitating binding of BubR1 but also by enhancing Cdc20 recruitment to kinetochores mediated by BubR1's internal Cdc20 binding site. Downstream of kinetochore-produced complexes, Bub3 promotes binding of BubR1's conserved, amino terminal Cdc20 binding domain to a site in Cdc20 that becomes exposed by initial Mad2 binding. This latter Bub3-stimulated event generates the final mitotic checkpoint complex of Bub3–BubR1–Cdc20 that selectively inhibits ubiquitination of securin and cyclin B by APC/C^{Cdc20}. Thus, Bub3 promotes two distinct BubR1–Cdc20 interactions, involving each of the two Cdc20 binding sites of BubR1 and acting at unattached kinetochores or cytoplasmically, respectively, to facilitate production of the mitotic checkpoint inhibitor.

Upon entry into mitosis, each duplicated chromosome aligns at metaphase through capture of spindle microtubules by the kinetochore assembled onto its centromere. Premature chromosome segregation often leads to abnormal chromosome number, or aneuploidy, a hallmark of cancer. The mitotic checkpoint (also known as the spindle assembly checkpoint) is the major cell-cycle control mechanism in mitosis. It functions to ensure accurate chromosome segregation through production of an inhibitory signal generated by unattached kinetochores (1), thereby delaying anaphase onset until all of the chromosomes attach to spindle microtubules (2–4). This signaling pathway is initiated by a complex of Mad1 (mitotic arrest deficient 1) and Mad2 (mitotic arrest deficient 2) immobilized at unattached kinetochores (5). This complex then recruits a second Mad2 molecule (5–7) and catalyzes (8–10) its conformational change from open or N1 (inactive) to closed or N2 (active) (11, 12) state. Closed Mad2 can bind Cdc20 (cell division cycle 20), the mitotic activator of the E3 ubiquitin ligase APC/C (anaphase promoting complex or cyclosome) that is responsible for advance to anaphase by its ubiquitination and subsequent proteasome-dependent degradation of cyclin B and securin. Diffusible Mad2–Cdc20 produced by unattached kinetochores recruits a complex of Bub3 (budding uninhibited by benzimidazole 3) and BubR1 (Bub1 related protein 1). It does this either by exposing a previously inaccessible site in Cdc20 for binding to BubR1's N-terminal Cdc20 binding domain (13) and/or by a direct interaction between Cdc20-bound Mad2 and BubR1 (14).

A four-protein complex of Mad2, BubR1, Bub3, and Cdc20, named the mitotic checkpoint complex (or MCC), has long been implicated in the inhibition of APC/C^{Cdc20} ubiquitination of securin and cyclin B1 (14, 15). However, the identity of the ultimate mitotic checkpoint inhibitor remains controversial, with some investigators arguing that Mad2 plays the predominant role (16) and others arguing that the inhibitory activity of APC/C^{Cdc20} is provided by BubR1 (13, 17), or both BubR1 and Mad2 (14, 15). We recently demonstrated that the N-terminal Mad3 homology domain of BubR1 (including one of its two Cdc20 binding

sites) (18), along with its associated Bub3, but not Mad2, accounts for the inhibition of APC/C^{Cdc20} both in vitro using purified components and in vivo after induced degradation of either BubR1 or Mad2 (13). These latter in vivo efforts were interpreted to demonstrate that Mad2 can dissociate from an initial complex with Cdc20 (or APC/C^{Cdc20}) in an activated conformation capable of catalyzing additional Bub3–BubR1–Cdc20 complexes. Thus, we proposed that BubR1–Bub3–Cdc20 is the mitotic checkpoint inhibitor that blocks APC/C-dependent ubiquitination of cyclin B and securin, through dual catalytic steps, an initial one at kinetochores and another acting within the cytoplasm mediated by kinetochore-derived, activated Mad2 (13).

Bub3 was identified as a mitotic checkpoint protein through genetic screening in budding yeast (19), and subsequent work in higher eukaryotes also demonstrated a profound defect in this checkpoint in the absence of Bub3 (20–23). Recently, Bub3 has been shown to bind the phospho MELT motif on KNL-1 for kinetochore localization of Bub1 (budding uninhibited by benzimidazole 1), disruption of which caused a defective checkpoint (24–27) with Bub1 binding to kinetochores apparently required for binding of other checkpoint proteins (28–32). A role for Bub3 in mitotic checkpoint silencing has also been proposed in fission yeast (33). Bub3 binds to the Gle2-binding-sequence (GLEBS) motif of Bub1 and Mad3 (the yeast homolog of BubR1) in a mutually exclusive manner, with binding mediated through the top face of its β -propeller (34). Another GLEBS motif-containing protein, BugZ, was also shown to interact with Bub3, stimulating its mitotic function by promoting its stability and kinetochore loading (35–37). Bub3 not only mediates BubR1

Significance

The mitotic checkpoint (or the spindle assembly checkpoint) ensures genome integrity by preventing premature chromosome segregation. The pathway is triggered locally by kinetochores, multiprotein complexes assembled onto centromeres. Unattached kinetochores produce Mad2 bound to Cdc20, the mitotic activator of the E3 ubiquitin ligase APC/C. The initial Mad2–Cdc20 complex is then converted into the final mitotic checkpoint inhibitor Bub3–BubR1–Cdc20 that blocks APC/C (anaphase promoting complex or cyclosome)-dependent ubiquitination of cyclin B and securin, thereby stabilizing them and preventing an advance to anaphase. In this study, we identify dual mechanisms by which Bub3 promotes mitotic checkpoint signaling. Bub3 binding to BubR1 promotes two distinct BubR1–Cdc20 interactions, one acting at unattached kinetochores and the other cytoplasmically to facilitate production of the mitotic checkpoint inhibitor.

Author contributions: J.S.H., B.V., D.F., and D.W.C. designed research; J.S.H., B.V., and D.F. performed research; J.S.H., B.V., D.F., and D.W.C. analyzed data; and J.S.H. and D.W.C. wrote the paper.

The authors declare no conflict of interest.

¹To whom correspondence may be addressed. Email: dcleveland@ucsd.edu or j3han@ucsd.edu.

²B.V. and D.F. contributed equally to this work.

This article contains supporting information online at www.pnas.org/lookup/suppl/doi:10.1073/pnas.1416277111/-DCSupplemental.

localization to the kinetochore (38) but is also incorporated into the MCC with Cdc20, BubR1, and Mad2 (15). Failure of Bub3 binding to BubR1 has been shown to weaken the mitotic checkpoint (39–41). However, it has remained unclear how Bub3 stimulates mitotic checkpoint signaling through binding to BubR1.

Using cell-based assays and our established *in vitro* reconstituted APC/C activity assay (8, 13), we now have investigated the mechanism by which Bub3 contributes to the mitotic checkpoint. We find that Bub3 promotes two distinct BubR1–Cdc20 interactions, involving each of the two Cdc20 binding sites of BubR1 and acting at unattached kinetochores or cytoplasmically, respectively, to facilitate production of the mitotic checkpoint inhibitor.

Results

Bub3 Directly Stimulates Production of the APC/C^{Cdc20} Inhibitor of Cyclin B Ubiquitination. To determine the specific contribution of Bub3 binding to BubR1 in the mitotic checkpoint, endogenous BubR1 was depleted in cells using an siRNA and replaced by expression of inducible, siRNA-resistant, Myc and GFP amino-terminally tagged BubR1 variants (Fig. S1C and Fig. 1A and B). To disrupt binding to Bub3, we converted the conserved glutamate at residue 409 of the GLEBS motif of BubR1 (34) to lysine. Depletion of Bub3 produced a severe defect in nocodazole-induced, chronic mitotic checkpoint signaling (Fig. S1A and B), as expected from prior work (23). The BubR1^{E409K} variant with a defect in Bub3 binding gave rise to extensive chromosome misalignment yet failed to delay anaphase onset in an unperturbed mitosis (Fig. S1D and E). Additionally, BubR1^{E409K} allowed much faster mitotic exit than wild-type BubR1 in cells with unattached kinetochores produced either by nocodazole-induced microtubule disassembly (Fig. 1C and D) or inhibition of the kinetochore-bound, kinesin family member CENP-E (Fig. S1F–H). Taken together, these results indicate that the Bub3–BubR1 interaction is required for sustained mitotic checkpoint signaling.

Bub3 has been copurified with BubR1 and Mad2 in Cdc20 complex(es) from cells with an active mitotic checkpoint (15, 17, 42), suggesting a contribution by Bub3 to the inhibition of Cdc20. To determine the direct contribution of Bub3 to the inhibition of APC/C^{Cdc20} *in vitro*, Bub3 and various combinations of full-length BubR1 (hereafter referred to as BubR1^{FL}) and Mad2 (Fig. 1E) were coinubated at concentrations approximating physiological (150, 150, and 300 nM, respectively) (8, 42). Mad2 and/or BubR1 were then added to bead-bound APC/C^{Cdc20} (at 2:1 or 1:1 stoichiometries, respectively, relative to Cdc20). APC/C and any associated proteins were recovered, and ubiquitination activity toward cyclin B substrate was assayed after addition of E1, the E2 UbcH10, and ubiquitin (see schematic in Fig. 1F). Incubation of Mad2 and BubR1^{FL} at levels approximating their known physiological concentrations partially suppressed APC/C^{Cdc20}-mediated cyclin B ubiquitination, as determined by quantifying unubiquitinated cyclin B (Fig. 1G, lane 6, H, and I). Although Bub3 alone or in combination with Mad2 produced no APC/C^{Cdc20} inhibition, when added with BubR1^{FL} and Mad2, it stimulated them to produce complete loss of cyclin B ubiquitination (Fig. 1G, lane 7, H, and I). Thus, Bub3 directly promotes the production of an APC/C^{Cdc20} inhibitor, independent of any function for it at kinetochores.

Bub3 Binding Enhances Inhibition of APC/C^{Cdc20} Mediated by the Mad3 Homology Region of BubR1. BubR1 contains two Cdc20 binding sites, a conserved site in the N-terminal Mad3–homology domain and an internal site that is present only in higher eukaryotes. The two Cdc20 binding sites of BubR1 have been shown to be able, respectively, to mediate inhibition of Cdc20 activation of APC/C in Mad2-dependent (13, 41) and Mad2-independent manners (42). We tested the contributions of the individual Cdc20 binding sites of BubR1 in Bub3-stimulated inhibition of APC/C^{Cdc20} ubiquitination of cyclin B *in vitro*. Bub3 enhanced inhibition of APC/C^{Cdc20}

mediated by BubR1_{1–477} (hereafter referred as BubR1^N), which contains BubR1's N-terminal Cdc20 binding site (Fig. 24). In contrast, Bub3 did not affect Mad2-independent inhibition by BubR1 of free Cdc20 activation of APC/C (inhibition mediated by a BubR1 variant [BubR1_{357–1050}] containing only its internal Cdc20 binding site—hereafter referred to as BubR1^C) (Fig. S2). This stimulated inhibition required a direct interaction between BubR1^N with Bub3, as Bub3 failed to activate Bub3 binding-defective BubR1^{N-E409K} (Fig. 2D–F). The E409K mutation itself did not affect function of BubR1, as there was no difference between wild-type BubR1^N and BubR1^{N-E409K} in their ability to inhibit APC/C^{Cdc20} in the absence of Bub3 (Fig. S3). Consistently, a Bub3 variant (Bub3^{R183E}) that contains a mutation of arginine 183 (corresponding to arginine 197 in yeast, a residue required for its interaction with Bub1 or Mad3) (34) bound less to BubR1^N and also produced a correspondingly reduced ability to stimulate BubR1^N inhibition of APC/C^{Cdc20} (Fig. S4). Collectively, these data indicate that Bub3 binding to BubR1 specifically promotes the Mad3–homology domain (BubR1^N)-mediated production of an APC/C^{Cdc20} inhibitor.

Bub3 Promotes Assembly of the BubR1–Cdc20 Mitotic Checkpoint Inhibitor. Our previous study found that BubR1 binding to Cdc20 (through the N-terminal Cdc20 binding domain), but not Mad2, is critical for inhibition of APC/C^{Cdc20} recognition of cyclin B (13). Because Bub3 stimulated the inhibition of APC/C^{Cdc20} by BubR1^N (Fig. 2), we therefore tested *in vitro* if Bub3 promoted BubR1^N association with Cdc20. Bead-bound APC/C^{Cdc20} was purified after incubating with various combinations of BubR1^N, Mad2, and Bub3, and APC/C-associated proteins were then analyzed (Fig. 3A; see schematic at top). BubR1^N, with or without Bub3, failed to produce a significant amount of BubR1^N–Cdc20 complex in the absence of Mad2 (Fig. 3A, lanes 3–5), indicating a Mad2 dependency for establishing an initial BubR1^N–Cdc20 interaction. This Mad2-dependent BubR1^N–Cdc20 interaction was enhanced by twofold by coinubation with Bub3 (Fig. 3A, lanes 6–8, and B), quantitatively accounting for the twofold stimulation of APC/C^{Cdc20} inhibition by Bub3 (Fig. 2C). We further confirmed that Bub3-stimulated inhibition required its binding to BubR1^N, as Bub3 was unable to promote APC/C^{Cdc20} association with a shorter BubR1^N variant lacking the Bub3 binding domain (BubR1_{1–363}) (Fig. 3C). Consistent with *in vitro* results, immunopurified BubR1^{E409K} (Bub3 binding-defective) from mitotically arrested cells was less associated with Cdc20 and APC/C than wild-type BubR1 (Fig. 3D and E).

Bub3-Mediated Kinetochore Recruitment of BubR1 Enhances Mitotic Checkpoint Signaling. Unattached kinetochores stably bind a complex of Mad1 and Mad2 (5), which catalytically acts (8, 10) to convert additional Mad2 molecules to an active form that binds Cdc20, thereby initiating mitotic checkpoint signaling. The other components of the MCC—BubR1, Bub3 (38), and Cdc20 (43)—are also recruited to unattached kinetochores (reviewed in ref. 44). Because BubR1 relies on Bub3 for its binding to kinetochore (38), we tested whether such Bub3-dependent targeting of BubR1 to kinetochores also promotes mitotic checkpoint signaling beyond kinetochore binding-independent Bub3 stimulation of BubR1–Cdc20 complex formation (Fig. 3). To produce kinetochore localization of the cytosolic BubR1^{E409K}, GFP-tagged Mis12 or Bub3, respectively, was fused in frame to the N or C terminus of the protein (Fig. 4A). After siRNA-mediated reduction in endogenous BubR1, these Bub3 and Mis12 fusion proteins accumulated to levels similar to that of the corresponding GFP-tagged BubR1 variants (Fig. 4B). As expected, BubR1^{E409K} was not kinetochore-associated unless fused to Bub3 or Mis12 (Fig. 4C).

Compared with BubR1^{E409K} alone, BubR1 significantly extended nocodazole-induced mitotic arrest in cells when kinetochore targeted through Bub3 but not Mis12 (Fig. 4D and E). BubR1 localization to the kinetochore per se was necessary for Bub3 enhancement of

mitotic checkpoint signaling, as the Bub3-dependent extended mitotic arrest largely disappeared (Fig. 4F) when BubR1^{E409K} was fused to a Bub3 variant (Bub3^{R183E}) defective in kinetochore localization (Fig. 4G). Although the Bub3 fusion enables kinetochore binding of BubR1^{E409K} through Bub3 binding to Bub1 at the kinetochore,

the E409K mutation in BubR1's GLEBS motif disrupts the authentic BubR1–Bub3 interaction between the fused Bub3 and BubR1^{E409K}. As a consequence, it is unlikely that Bub3 fusion to the C terminus of BubR1^{E409K} directly facilitates BubR1 binding to APC/C^{Cdc20}.

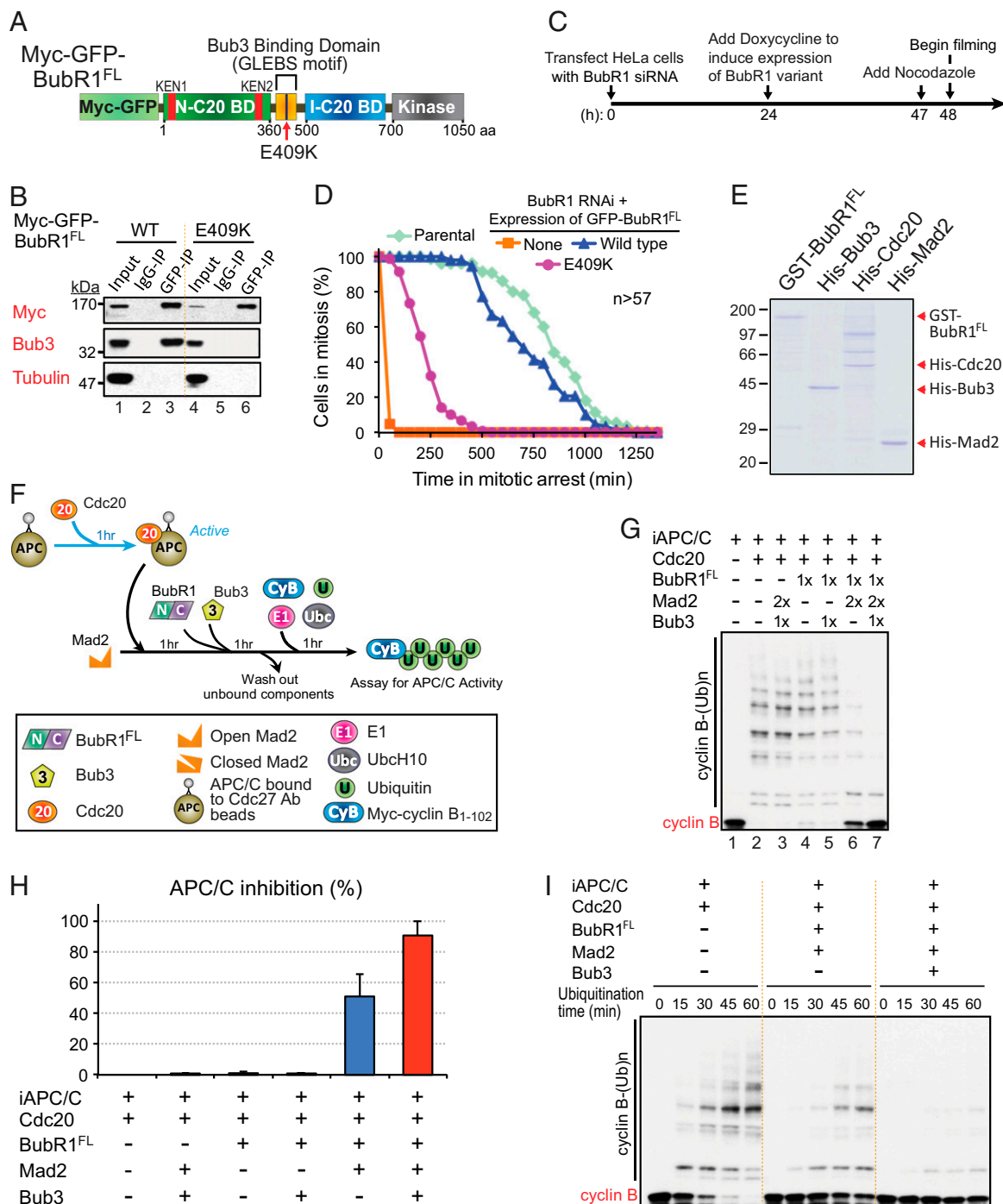


Fig. 1. Bub3 directly promotes Mad2-dependent BubR1 inhibition of APC/C. (A) Schematic of functional domains of BubR1. (B) E409K mutation in BubR1 disrupts the BubR1–Bub3 interaction, analyzed by GFP immunoprecipitation. (C) Schematic for the protocol used to replace endogenous BubR1 with a GFP-tagged version and to determine duration of nocodazole-induced mitotic arrest in HeLa cells. (D) Time-lapse microscopy was used to determine nocodazole (100 ng/mL)-induced mitotic duration after replacing endogenous BubR1 with GFP–BubR1 variants using siRNA. (E) Coomassie staining of purified checkpoint components. (F) In vitro APC/C activity assay for checkpoint protein-mediated inhibition of APC/C-mediated cyclin B ubiquitination. (G) Effect on APC/C^{Cdc20}-mediated ubiquitination of cyclin B_{1–102} by various combinations of BubR1, Mad2, and Bub3. (H) Quantification from G. Data represent mean \pm SEM, $n = 3$. (I) Time titration for the inhibition of APC/C ubiquitination of cyclin B by Mad2 and BubR1 in the presence or absence of Bub3.

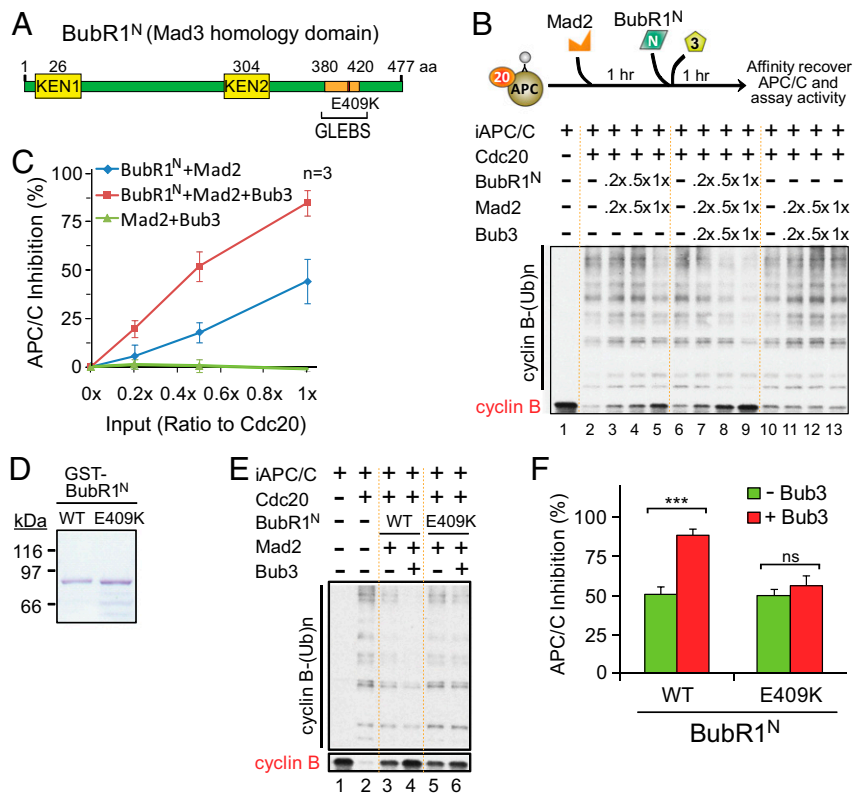


Fig. 2. Bub3 binding promotes the conserved N-terminal Mad3 homology domain of BubR1-mediated inhibition of APC/C^{Cdc20}. (A) Schematic for the Mad3 homology domain of BubR1 (BubR1^N, 1–477 aa). (B) Inhibition of APC/C^{Cdc20} activity by various combinations of checkpoint proteins. (C) Quantification from B. (D) Coomassie staining of purified wild-type or E409K mutant BubR1^N. (E) Test for requirement of Bub3 binding to BubR1 for Bub3 stimulation of BubR1^N. (F) Quantification from E. Data represent mean \pm SEM. *** $P < 0.001$ from Student *t* test.

Despite kinetochore binding-derived stimulation of sustained checkpoint signaling, cells expressing Bub3-tagged BubR1^{E409K} exited mitosis in nocodazole significantly faster than cells expressing wild-type BubR1 (Fig. 4E, compare blue and purple lines). Thus, we reasoned that the kinetochore binding-independent Bub3 stimulation of the BubR1–Cdc20 interaction documented earlier (Fig. 3) was necessary for sustained mitotic checkpoint signaling. In support of this, wild-type BubR1 fused to Bub3 or Mis12 instead of BubR1^{E409K} mediated an even further extension of mitotic arrest regardless of the way it was bound to kinetochores (Fig. S5).

Next, we asked whether kinetochore localization of the N-terminal Cdc20 binding site of BubR1 was sufficient for its kinetochore localization-dependent enhancement of mitotic checkpoint signaling. A GFP-tagged N-terminal BubR1 variant (BubR1_{1–363} that lacks the Bub3 binding site) was directly fused to Bub3 or Mis12 (Fig. 5A). After suppressing endogenous BubR1 with siRNA, each Bub3 or Mis12 fusion protein accumulated to a level similar to untagged BubR1_{1–363} (Fig. 5B). Bub3- and Mis12-tagged BubR1_{1–363} variants bound to kinetochores, whereas BubR1_{1–363} did not (Fig. 5C). Both full-length BubR1 and the Bub3–BubR1_{1–363} fusion bound dynamically, with similar turnover kinetics measured by fluorescence recovery after photo bleaching (FRAP) during nocodazole-induced mitotic arrest (Fig. 5D, E, and G). In contrast, FRAP measurements with Mis12-tagged BubR1_{1–363} revealed it to be bound stably to kinetochores, with little exchange with time (Fig. 5F and G). However, unlike full-length cytosolic BubR1 (BubR1^{E409K}) (Fig. 4E), neither enabling dynamic nor stable association of BubR1_{1–363} with kinetochores extended the time of nocodazole-induced mitotic arrest (Fig. 5H and I). This indicates a requirement for additional domains of BubR1 for kinetochore binding-dependent enhancement of sustained mitotic checkpoint signaling.

The Internal Cdc20 Binding Site of BubR1 Accelerates Cdc20 Recruitment to Kinetochores. Full-length BubR1 has been shown (13) to sustain more robust mitotic checkpoint signaling than the kinetochore localization-competent variant BubR1^N, which contains the Bub3 and N-terminal Cdc20 binding sites but is missing the internal Cdc20 binding site and the kinase domain. Although the role of the BubR1 kinase domain remains controversial [with evidence that kinase activity is stimulated by binding to CENP-E (45) and conflicting with evidence that it is an inactive pseudokinase (46)], BubR1 has been recently proposed to be required for Cdc20 recruitment to the *Drosophila melanogaster* kinetochore (47, 48). These findings led us to test whether BubR1 localization to the kinetochore enhances recruitment of Cdc20 to kinetochores in human cells. Using siRNA we replaced endogenous BubR1 with an siRNA-resistant MycGFP–BubR1 variant and measured Cdc20 intensity at the kinetochore during mitotic arrest produced by addition of monastrol, an inhibitor for the mitotic kinesin Eg5. Cdc20 intensity at the kinetochore was reduced at least 75% upon depletion of endogenous BubR1 (Fig. 6A and B). Expression of recombinant wild-type BubR1 or the kinetochore binding-competent BubR1 variant (BubR1^{E409K}–Bub3) fully restored the Cdc20 level at kinetochores, whereas expression of the kinetochore binding-deficient BubR1 variant (BubR1^{E409K}) did not.

Next, we assessed the contribution to kinetochore binding of Cdc20 and to sustained mitotic checkpoint arrest provided by each of the two Cdc20 binding sites of BubR1. Expression of a BubR1 variant lacking the N-terminal Cdc20 binding site [BubR1 Δ (1–356)] fully restored Cdc20 levels at kinetochores in BubR1-depleted cells. On the other hand, expression of a BubR1 variant lacking the internal Cdc20 binding site [BubR1 Δ (525–700)] did not (Fig. 6C and D). Importantly, wild-type BubR1 mediated

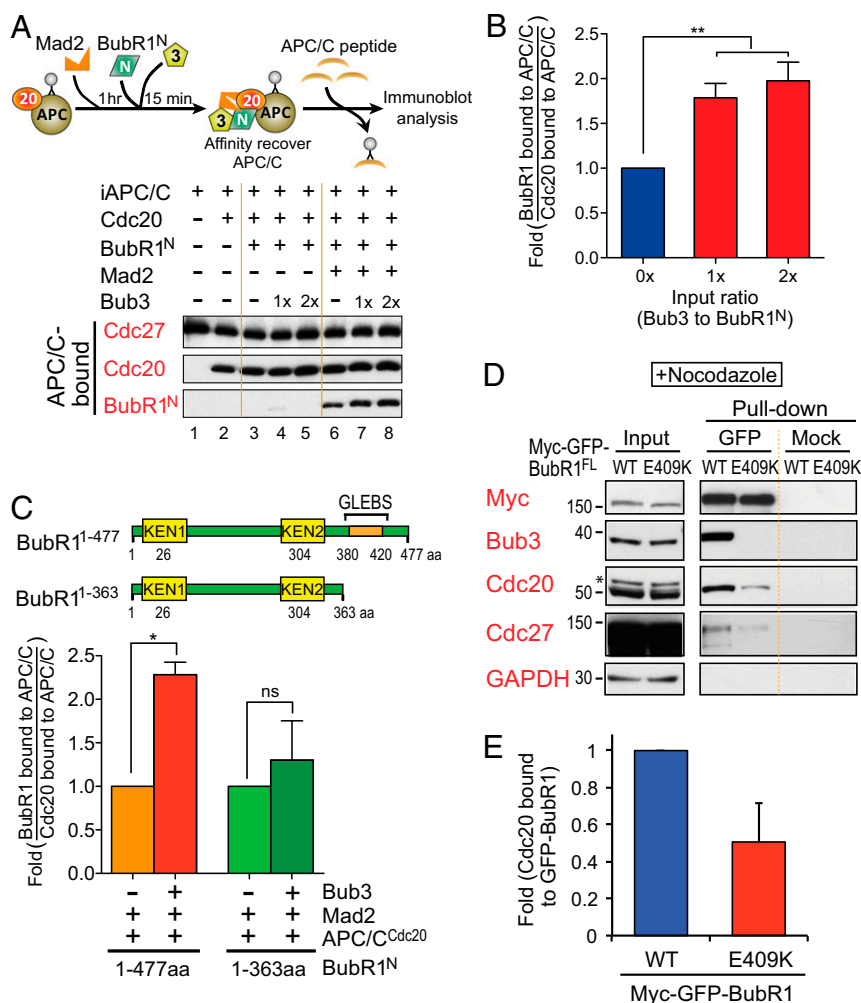


Fig. 3. Bub3 binding promotes the Mad2-dependent N-terminal Mad3 homology domain of BubR1 binding to Cdc20. (A) In vitro assay of Bub3-dependent effects on binding of APC/C-bound Cdc20 to the N-terminal Cdc20 binding site of BubR1. (B) Quantification from A. (C) In vitro test if Bub3 stimulation of the BubR1–Cdc20 interaction in A required the Bub3 binding domain of BubR1. (D) Assay (using GFP immunoprecipitation of extracts from nocodazole-induced mitotic HeLa cells) to measure E409K GFP-BubR1 mutant association with Bub3, Cdc20, and the APC/C subunit Cdc27. (E) Quantification from D. Data represent mean \pm SEM. * $P < 0.05$ and ** $P < 0.01$ from Student *t* test, $n = 3$.

longer mitotic arrest of nocodazole-treated cells than did BubR1 $\Delta(525-700)$ (Fig. 6E), suggesting a role of BubR1–Bub3-mediated kinetochore binding of Cdc20 in sustaining mitotic checkpoint signaling. Kinetochore levels of Mad1 and Mad2 were indistinguishable in cells supported by the various BubR1 variant regardless of the levels of kinetochore binding of BubR1 or Cdc20 (Fig. S6). This outcome was inconsistent with the possibility that a less efficient Mad1–Mad2-mediated initiation of checkpoint signaling was the result of reduction in Mad1–Mad2 at unattached kinetochores.

Discussion

A prevailing hypothesis for Bub3's function in generation of the mitotic checkpoint inhibitor is that it simply delivers BubR1 to the kinetochore and thus elevates the local concentration of BubR1 to facilitate rapid initial production of an anaphase inhibitor (e.g., refs. 2, 40, 49). Here we have established that Bub3's role is much more than this. Our evidence identifies a dual mode of stimulation by Bub3 of BubR1's mitotic checkpoint function to produce the mitotic checkpoint inhibitor (modeled in Fig. 6F). First, Bub3's binding to BubR1 directly stimulates assembly of the BubR1–Cdc20 mitotic checkpoint inhibitor through facilitating association of the conserved Mad3–homology domain of BubR1

with Cdc20 independently of kinetochore localization. Second, we have further demonstrated that Bub3 binding also mediates Cdc20 localization to the kinetochore via BubR1's internal Cdc20 binding site as a means to reinforce the kinetochore-dependent first step in mitotic checkpoint inhibitor generation.

Recently, we demonstrated that BubR1, but not Mad2, binding (through the N-terminal Cdc20 binding site) is critical for inhibiting APC/C^{Cdc20} recognition of cyclin B (13). Our evidence in the current study has established that Bub3 promotes this BubR1–Cdc20 interaction, thereby uncovering a previously unknown role for Bub3 in production of the mitotic checkpoint inhibitor through action at the most downstream step of the signaling pathway. Two previous studies proposed that the first KEN box in the N-terminal Cdc20 binding site of BubR1 is responsible for BubR1 binding to Cdc20 (14, 41). Based on this, it is plausible that Bub3 binding may alter the conformation of the initially rod-shaped BubR1 N terminus (34, 50) in a way to either promote the initial assembly or stabilization of a BubR1–Cdc20 complex for generating the characteristic, selective inhibition of APC/C^{Cdc20}.

In addition to its stimulatory function in cytosolic assembly of the mitotic checkpoint inhibitor (Figs. 1 and 2), our evidence establishes that Bub3 also mediates BubR1-dependent kinetochore

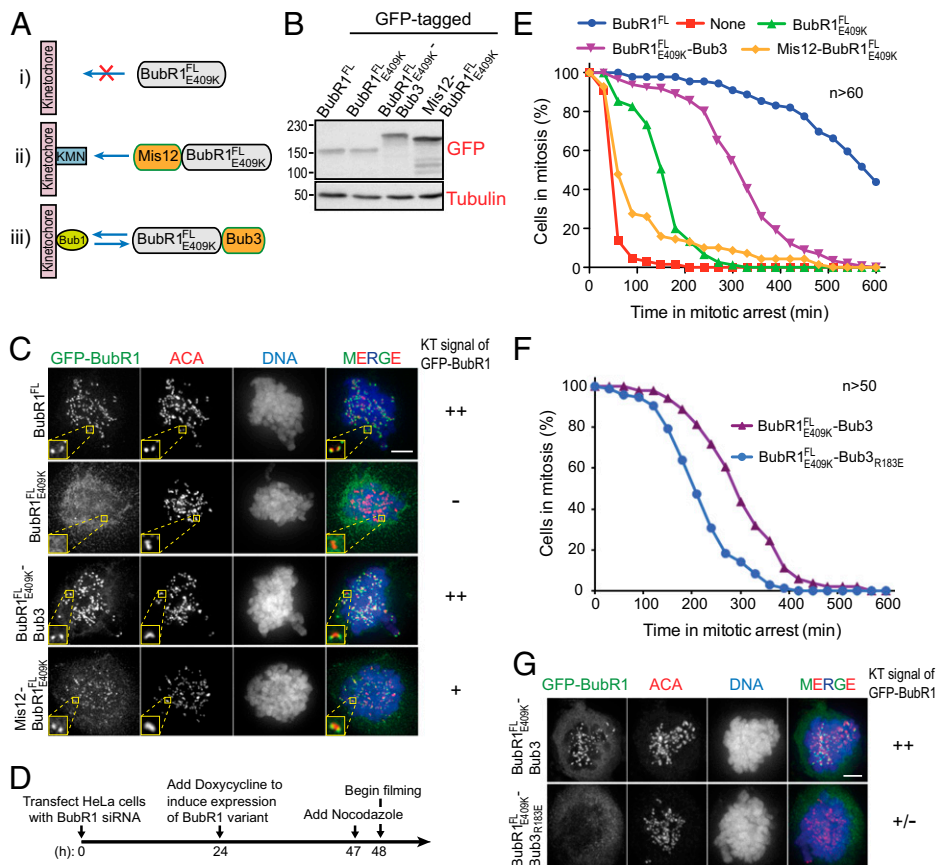


Fig. 4. Enabling a cytosolic BubR1 to localize dynamically to the kinetochore enhances mitotic checkpoint signaling. (A) Schematic showing three tests for assessing BubR1's role at kinetochores, including (i) blocking BubR1 binding at kinetochores with the E409K mutation, (ii) tethering BubR1 to kinetochores by fusion to Mis12, and (iii) directly tethering BubR1 to Bub3 to mediate kinetochore association. (B) Levels of accumulation of various GFP-BubR1 variants after expression in HeLa cells. (C) Localization of BubR1^{FL} or Bub3 or Mis12-tagged cytosolic BubR1^{E409K}. (D) Schematic of the protocol used in E to determine duration of nocodazole-induced mitotic arrest in cells expressing recombinant BubR1 variants. (E) Test of mitotic checkpoint function of various BubR1 variants. Time-lapse microscopy was used to determine nocodazole-induced mitotic duration after replacing endogenous BubR1 with GFP-BubR1 variants using siRNA. (F) Quantitation of mitotic timing in individual cells assayed as in E. (G) Indirect immunofluorescence to assess kinetochore binding of BubR1^{E409K} fused to Bub3 with or without an additional R183E mutation in Bub3.

recruitment of Cdc20 as a means to further strengthen initiation of mitotic checkpoint inhibitor production (Fig. 6F). How BubR1 and Cdc20 recruitment to kinetochores serves to power checkpoint signaling is not settled, with two (not mutually exclusive) mechanisms likely. First, recruitment at kinetochores of Cdc20 by BubR1's internal Cdc20 binding site may facilitate initial formation of Mad2-Cdc20 complexes whose assembly is enhanced by the elevated local concentration at those kinetochores of Cdc20. Alternatively, the internal Cdc20 binding site may serve as a docking site of preassembled Mad2-Cdc20 for its handover to the N-terminal Cdc20 binding site of BubR1 for the assembly of the BubR1-Cdc20 mitotic checkpoint inhibitor. Evaluating between these hypotheses will now require testing (i) whether the two Cdc20 binding sites of BubR1 associate with Cdc20 independently of each other, including whether a transient complex forms in which both Cdc20 binding sites are associated with one molecule of Cdc20 as an intermediate form, and (ii) whether the internal Cdc20 binding site of BubR1 binds to Mad2-Cdc20.

Our study has further revealed that BubR1's diffusion into the cytosol, as well as its kinetochore localization, is crucial for mitotic checkpoint signaling, as indicated by the fact that tethering cytosolic BubR1 (BubR1^{E409K}) stably to the kinetochore (via Mis12) was even more detrimental to mitotic checkpoint signaling than was keeping BubR1 only in the cytosol (Fig. 4E). By contrast, enabling dynamic attachment of an otherwise cytosolic

BubR1 variant to the kinetochore (by fusing it to Bub3) significantly strengthened sustained mitotic checkpoint signaling (Fig. 4E). This evidence adds further support for our model for production of a diffusible mitotic checkpoint inhibitor in which the majority of Mad2-associated Cdc20 complexes diffuse throughout the mitotic cytoplasm, followed by capture by cytosolic BubR1 to produce the bona fide inhibitor of APC/C^{Cdc20} recognition of cyclin B and securin (13).

Finally, we note that BubR1 at the unattached kinetochores has been reported to recruit PP2A-B56 α , which in turn affects kinetochore-microtubule attachment (51–53) through a region similar to the one required for its recruitment of Cdc20 for mitotic checkpoint signaling. This raises an interesting, now testable, possibility that there is crosstalk between these two distinct protein-protein interactions at kinetochores, one to initiate mitotic checkpoint signaling and the other to coordinate microtubule-kinetochore attachment to silence that signaling.

Materials and Methods

Constructs. Full-length and fragments of the human BubR1 ORF were cloned into either a pcDNA5/FRT (FLP recombination target)/TO (tetracycline resistance operon)-based vector (Invitrogen) modified to contain an amino-terminal Myc-LAP epitope tag for mammalian cell expression or a pFastBac1-based vector (Invitrogen) modified to contain an amino-terminal GST-human rhinovirus (HRV) 3C site for insect cell expression. The LAP tag consists of GFP-HRV 3C (LELVFQGP)-6xHis. All other DNA constructs were previously described (8, 42).

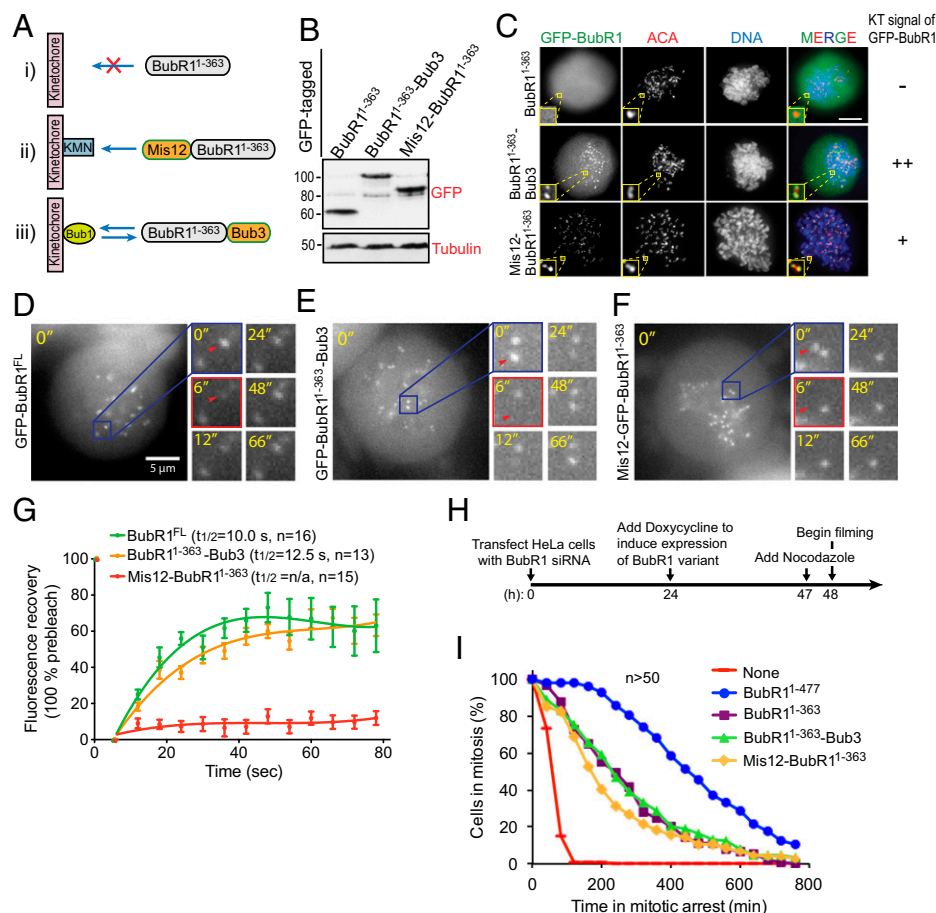


Fig. 5. Targeting a cytosolic BubR1 variant with only its N-terminal Cdc20 binding site to kinetochores does not enhance mitotic checkpoint signaling. (A) Schematics for (i) blocking BubR1^N (BubR1₁₋₃₆₃) binding to kinetochores by deleting the Bub3 binding site or by driving its kinetochore localization through fusion to (ii) Mis12 or (iii) Bub3. (B) Levels of accumulation of GFP-BubR1 variants after expression in HeLa cells. (C) Intracellular localization of Bub3 or Mis12-tagged cytosolic BubR1₁₋₃₆₃. (D–F) FRAP analysis of GFP-BubR1 variants in a nocodazole-induced mitotic cell. (D) Wild-type GFP-BubR1, (E) GFP-BubR1₁₋₃₆₃-Bub3, and (F) GFP-Mis12-BubR1₁₋₃₆₃. (G) Quantification from D–F. n/a, not available; t_{1/2}, time (seconds) for 50% recovery of fluorescence. (H) Schematic for the protocol used to determine mitotic timing. (I) Mitotic checkpoint function of BubR1 N terminus variants, analyzed by time-lapse microscopy.

Antibodies. The antibodies used in this study are as follows: BubR1 (SBR1.1, a gift from S. Taylor (University of Manchester, Manchester, England); A300-386, Bethyl Laboratories), Bub3 (SB3.2, a gift from S. Taylor), Mad2 (A300-300A, Bethyl Laboratories), Cdc20 [A301-180A, Bethyl Laboratories; SC-13162, Santa Cruz Biotechnology (for immunofluorescence)], Mad1 (BB3-8, a gift from A. Musacchio, Max Planck Institute, Dortmund, Germany), ACA (Antibodies Inc.), Myc (16-213, Millipore), Cdc27 (54), α -Tubulin (DM1 α , Sigma-Aldrich), GST (SC-33613, Santa Cruz Biotechnology), and His (A00186, GenScript).

Generation of Stable Cell Lines and RNAi. Parental Flp-In TRex-HeLa or -DLD-1 parental cells that stably express mRFP-tagged histone H2B (H2B-mRFP) were as previously described (55, 56). Stable, isogenic cell lines expressing MycGFP-BubR1 were generated using FRT/Flp-mediated recombination (57). Expression of MycGFP-BubR1 was induced with 1 μ g/mL tetracycline. siRNAs directed against the 3' untranslated region of BubR1 (5'-CUGUAUGUCU-GUAAUUUA-3') or Bub3 (58) were purchased from Thermo Fisher Scientific (Dharmacon). Cells were transfected with 50 nM of oligonucleotides using Lipofectamine RNAiMAX (Invitrogen). We added tetracycline 24 h after transfection to express MycGFP-BubR1 for 24 h before collecting cells for immunoblotting or analyzing by time-lapse microscopy.

Live-Cell Microscopy. To determine mitotic timing, cells were seeded onto μ -Slide (ibidi) and 48 h posttransfection transferred to supplemented CO₂-independent media (Invitrogen). Cells were maintained at 37 °C in an environmental control station and images collected using a Deltavision RT system (Applied Precision) with a 40 \times 1.35 NA oil lens at 3–5-min time intervals. For each time point, 6 \times 3 μ m or 6 \times 4 μ m z sections were acquired for RFP and maximum intensity

projection created using softWoRx. Movies were assembled and analyzed using QuickTime (Apple) or FIJI (Image J, National Institutes of Health) software.

FRAP. The FRAP experiment was performed on HeLa Cells seeded 24 h before the experiment in 35-mm glass-bottom culture dishes (Mat Tek Corporation). Growth medium was changed to CO₂-independent medium before imaging. Images were collected, at 37 °C, with an Olympus 100X/1.35, UPlan Apo objective using a DeltaVision Core system (Applied Precision) equipped with a Coolsnap camera (Roper). Photobleaching was performed using a Quantifiable Laser Module (Applied Precision) with the 488-nm laser line. Images were taken on a single plane, on the GFP channel, every second before the laser event. A 1-s laser event was performed, and images were acquired with increasing time interval following photo bleaching starting with 500-ms intervals. Fluorescent intensity was measured, using FIJI (ImageJ, National Institutes of Health), in a circle surrounding the GFP kinetochore signal, and a background was measured from an equivalent area adjacent to the kinetochore signal. Background subtraction and normalization of the measured signal was done using Excel software (Microsoft). The fitting of the data was done using Prism software (GraphPad), using a least square polynomial equation, and the recovery half-time was measured from the curve.

Indirect Immunofluorescence. Cells were fixed in 4% (vol/vol) formaldehyde at room temperature for 10 min with or without preextraction by 0.1% Triton X-100 for 60 s. Incubations with primary antibodies were conducted in blocking buffer for 1 h at room temperature. Immunofluorescence images were collected using a Deltavision Core system (Applied Precision). For quantification of kinetochore signal intensity, undeconvolved 2D maximum intensity projections were saved as unscaled 16-bit tagged image file format (TIFF) images and signal

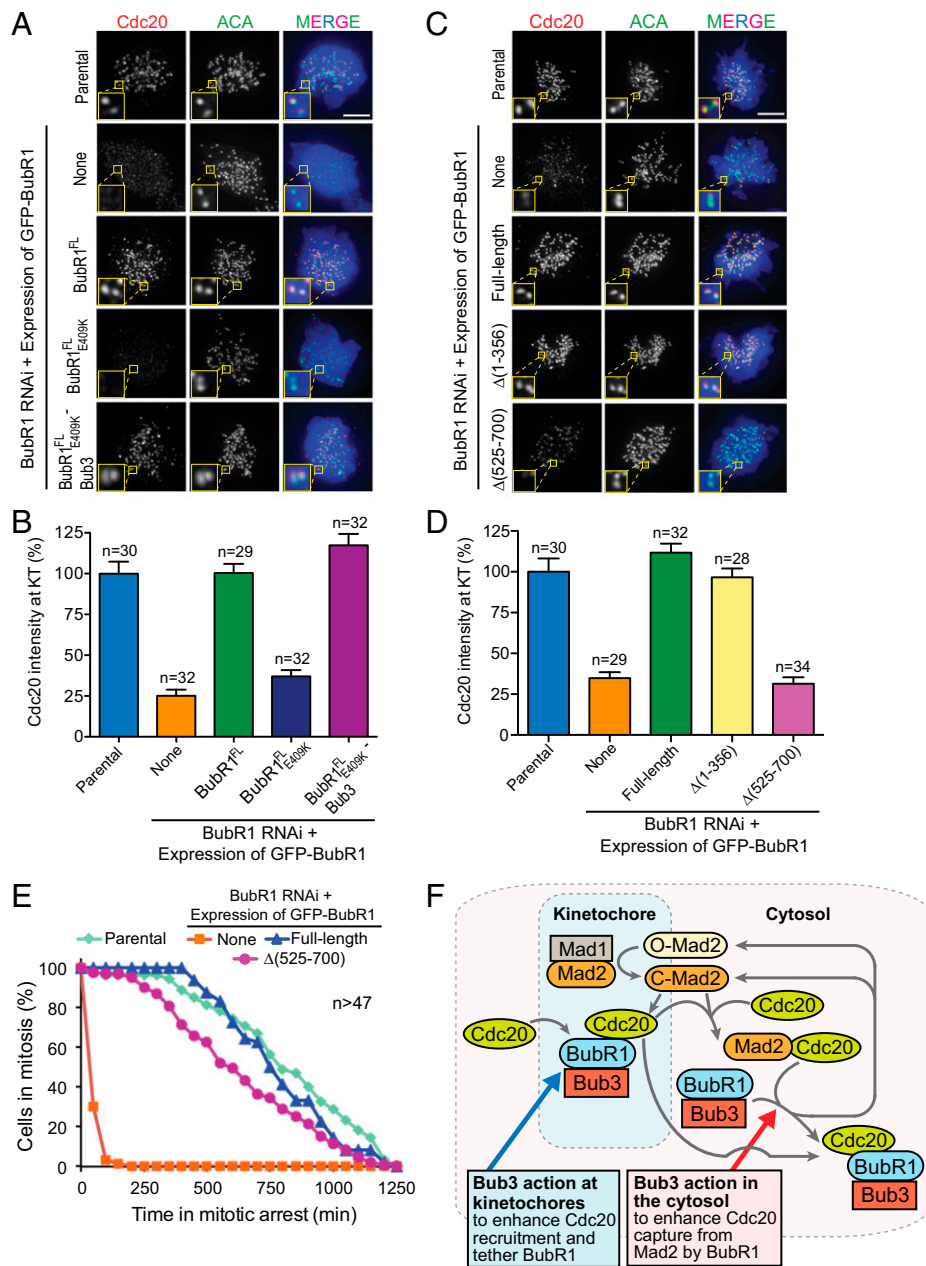


Fig. 6. Bub3 mediates kinetochore recruitment of Cdc20 via BubR1's internal Cdc20 binding site to enhance mitotic checkpoint signaling. (A) Effect of kinetochore localization of BubR1 on kinetochore localization of Cdc20 in HeLa cells arrested in mitosis with monastrol (100 μ M). (B) Quantification of Cdc20 intensity on kinetochores from A. (C) Indirect immunofluorescence assay of Cdc20 binding to kinetochores in the presence of BubR1 variants with either of its Cdc20 binding sites. (D) Quantification of Cdc20 intensity on kinetochores from C. (E) Duration of mitosis after reducing endogenous BubR1 (with siRNA) and expression of BubR1^{FL} or BubR1 deleted in its internal Cdc20 binding site. Time-lapse microscopy was used to determine nocodazole-induced duration of mitotic arrest after replacing endogenous BubR1 with a MycGFP-BubR1 in DLD-1 cells. (F) A model for dual modes of BubR1 activation by Bub3 for generating the mitotic checkpoint inhibitor. Mitotic checkpoint signaling is promoted (a) at kinetochores by Bub3-dependent recruitment to those kinetochores of BubR1 and Cdc20 (through binding of the internal Cdc20 binding site of BubR1 to Cdc20) and (b) in the cytosol by Bub3 stimulation of Mad2-dependent BubR1-Cdc20 formation (through binding of the conserved N-terminal Cdc20 binding site of BubR1).

intensities determined using MetaMorph (Molecular Devices). A 12 \times 12 pixel circle was drawn around a centromere [marked by anti-centromere antibodies (ACA) staining] and an identical circle drawn adjacent to the structure (background). The integrated signal intensity of each individual centromere was calculated by subtracting the fluorescence intensity of the background from the intensity of the adjacent centromere. About 20 centromeres were averaged to provide the average fluorescence intensity for each individual cell.

Protein Purification. GST or His-tagged human BubR1, Bub3, and Cdc20 were expressed in Sf9/High-Five insect cells using the Bac-to-Bac expression system

(Invitrogen) and affinity purified over nickel-nitrilotriacetic acid beads (Qiagen) or Glutathione Sepharose beads (GE Healthcare Life Sciences). His-Mad2 and other GST-tagged proteins were expressed from Rosetta *Escherichia coli* after induction with isopropyl beta-D-1-thiogalactopyranoside, and purified. APC/C was immunoprecipitated from interphase *Xenopus* egg extracts as previously described (8).

APC/C Ubiquitination Activity Assay. The APC/C ubiquitination activity assay was performed as previously described (59) and activity assessed by ubiquitination-derived depletion of the cyclin B₁₋₁₀₂ substrate. Quantitative

analysis of cyclin B₁₋₁₀₂ depletion was performed as previously described (13). Briefly, the level of cyclin B₁₋₁₀₂ was determined against a series of dilution of the proteins.

APC/C Binding Assay. APC/C was immunoprecipitated from *Xenopus* interphase egg extracts for 2 h at 4 °C using a peptide-derived anti-Cdc27 antibody crosslinked to Affiprep Protein A (Bio-Rad) beads. The APC/C beads were washed with Tris-buffered saline (TBS) buffer supplemented with 0.4 M KCl and 0.1% Triton X-100 and incubated with Cdc20 and checkpoint proteins sequentially or simultaneously for the indicated time at room temperature. Unbound proteins were removed by washing the beads twice with 20 volumes

of TBS buffer. The APC/C complex was eluted from the beads by Cdc27 peptide competition (2 mg/mL) as described and analyzed by immunoblotting.

ACKNOWLEDGMENTS. We thank Hongtao Yu, Stephen Taylor, and Andrea Musacchio for providing reagents and Jennifer Santini of the University of California, San Diego Neuroscience Microscopy Shared Facility (National Institute of Neurological Disorders and Stroke P30 NS047101). B.V. and D.F. were supported in part by postdoctoral fellowships from the Human Frontiers Science Program and the European Molecular Biology Organization, respectively. This work was supported by National Institutes of Health Grant GM20513 (to D.W.C.). Salary support for D.W.C. was provided by the Ludwig Institute for Cancer Research.

- Skibbens RV, Rieder CL, Salmon ED (1995) Kinetochores motility after severing between sister centromeres using laser microsurgery: Evidence that kinetochores directional instability and position is regulated by tension. *J Cell Sci* 108(Pt 7):2537–2548.
- Lara-Gonzalez P, Westhorpe FG, Taylor SS (2012) The spindle assembly checkpoint. *Curr Biol* 22(22):R966–R980.
- Jia L, Kim S, Yu H (2013) Tracking spindle checkpoint signals from kinetochores to APC/C. *Trends Biochem Sci* 38(6):302–311.
- Foley EA, Kapoor TM (2013) Microtubule attachment and spindle assembly checkpoint signalling at the kinetochore. *Nat Rev Mol Cell Biol* 14(1):25–37.
- Shah JV, et al. (2004) Dynamics of centromere and kinetochore proteins; implications for checkpoint signaling and silencing. *Curr Biol* 14(11):942–952.
- De Antoni A, et al. (2005) The Mad1/Mad2 complex as a template for Mad2 activation in the spindle assembly checkpoint. *Curr Biol* 15(3):214–225.
- Vink M, et al. (2006) In vitro FRAP identifies the minimal requirements for Mad2 kinetochore dynamics. *Curr Biol* 16(8):755–766.
- Kulikian A, Han JS, Cleveland DW (2009) Unattached kinetochores catalyze production of an anaphase inhibitor that requires a Mad2 template to prime Cdc20 for BubR1 binding. *Dev Cell* 16(1):105–117.
- Lad L, Lichtsteiner S, Hartman JJ, Wood KW, Sakowicz R (2009) Kinetic analysis of Mad2-Cdc20 formation: Conformational changes in Mad2 are catalyzed by a C-Mad2-ligand complex. *Biochemistry* 48(40):9503–9515.
- Simonetta M, et al. (2009) The influence of catalysis on mad2 activation dynamics. *PLoS Biol* 7(1):e10.
- Luo X, Yu H (2008) Protein metamorphosis: The two-state behavior of Mad2. *Structure* 16(11):1616–1625.
- Mapelli M, Musacchio A (2007) MAD conortions: Conformational dimerization boosts spindle checkpoint signaling. *Curr Opin Struct Biol* 17(6):716–725.
- Han JS, et al. (2013) Catalytic assembly of the mitotic checkpoint inhibitor BubR1-Cdc20 by a Mad2-induced functional switch in Cdc20. *Mol Cell* 51(1):92–104.
- Chao WC, Kulkarni K, Zhang Z, Kong EH, Barford D (2012) Structure of the mitotic checkpoint complex. *Nature* 484(7393):208–213.
- Sudakin V, Chan GK, Yen TJ (2001) Checkpoint inhibition of the APC/C in HeLa cells is mediated by a complex of BUBR1, BUB3, CDC20, and MAD2. *J Cell Biol* 154(5):925–936.
- Lau DT, Murray AW (2012) Mad2 and Mad3 cooperate to arrest budding yeast in mitosis. *Curr Biol* 22(3):180–190.
- Nilsson J, Yekezare M, Minshull J, Pines J (2008) The APC/C maintains the spindle assembly checkpoint by targeting Cdc20 for destruction. *Nat Cell Biol* 10(12):1411–1420.
- Murray AW, Marks D (2001) Can sequencing shed light on cell cycling? *Nature* 409(6822):844–846.
- Hoyt MA, Totis L, Roberts BT (1991) S. cerevisiae genes required for cell cycle arrest in response to loss of microtubule function. *Cell* 66(3):507–517.
- Kalitsis P, Earle E, Fowler KJ, Choo KH (2000) Bub3 gene disruption in mice reveals essential mitotic spindle checkpoint function during early embryogenesis. *Genes Dev* 14(18):2277–2282.
- Campbell L, Hardwick KG (2003) Analysis of Bub3 spindle checkpoint function in *Xenopus* egg extracts. *J Cell Sci* 116(Pt 4):617–628.
- Lopes CS, Sampaio P, Williams B, Goldberg M, Sunkel CE (2005) The *Drosophila* Bub3 protein is required for the mitotic checkpoint and for normal accumulation of cyclins during G2 and early stages of mitosis. *J Cell Sci* 118(Pt 1):187–198.
- Logarinho E, Resende T, Torres C, Bousbaa H (2008) The human spindle assembly checkpoint protein Bub3 is required for the establishment of efficient kinetochore-microtubule attachments. *Mol Biol Cell* 19(4):1798–1813.
- Primorac I, et al. (2013) Bub3 reads phosphorylated MELT repeats to promote spindle assembly checkpoint signaling. *eLife* 2:e01030.
- Shepperd LA, et al. (2012) Phosphodependent recruitment of Bub1 and Bub3 to Spc7/KNL1 by Mph1 kinase maintains the spindle checkpoint. *Curr Biol* 22(10):891–899.
- Yamagishi Y, Yang CH, Tanno Y, Watanabe Y (2012) MPS1/Mph1 phosphorylates the kinetochore protein KNL1/Spc7 to recruit SAC components. *Nat Cell Biol* 14(7):746–752.
- London N, Ceto S, Ranish JA, Biggins S (2012) Phosphoregulation of Spc105 by Mps1 and PP1 regulates Bub1 localization to kinetochores. *Curr Biol* 22(10):900–906.
- Johnson VL, Scott MI, Holt SV, Hussein D, Taylor SS (2004) Bub1 is required for kinetochore localization of BubR1, Cenp-E, Cenp-F and Mad2, and chromosome congression. *J Cell Sci* 117(Pt 8):1577–1589.
- Kim S, Sun H, Tomchick DR, Yu H, Luo X (2012) Structure of human Mad1 C-terminal domain reveals its involvement in kinetochore targeting. *Proc Natl Acad Sci USA* 109(17):6549–6554.
- Moyle MW, et al. (2014) A Bub1-Mad1 interaction targets the Mad1-Mad2 complex to unattached kinetochores to initiate the spindle checkpoint. *J Cell Biol* 204(5):647–657.
- Heinrich S, et al. (2014) Mad1 contribution to spindle assembly checkpoint signalling goes beyond presenting Mad2 at kinetochores. *EMBO Rep* 15(3):291–298.
- London N, Biggins S (2014) Mad1 kinetochore recruitment by Mps1-mediated phosphorylation of Bub1 signals the spindle checkpoint. *Genes Dev* 28(2):140–152.
- Vanoosthuysen V, Meadows JC, van der Sar SJ, Millar JB, Hardwick KG (2009) Bub3p facilitates spindle checkpoint silencing in fission yeast. *Mol Biol Cell* 20(24):5096–5105.
- Larsen NA, Al-Bassam J, Wei RR, Harrison SC (2007) Structural analysis of Bub3 interactions in the mitotic spindle checkpoint. *Proc Natl Acad Sci USA* 104(4):1201–1206.
- Ji Z, Yu H (2014) A protective chaperone for the kinetochore adaptor Bub3. *Dev Cell* 28(3):223–224.
- Jiang H, et al. (2014) A microtubule-associated zinc finger protein, BuGZ, regulates mitotic chromosome alignment by ensuring Bub3 stability and kinetochore targeting. *Dev Cell* 28(3):268–281.
- Toledo CM, et al. (2014) BuGZ is required for Bub3 stability, Bub1 kinetochore function, and chromosome alignment. *Dev Cell* 28(3):282–294.
- Taylor SS, Ha E, McKeon F (1998) The human homologue of Bub3 is required for kinetochore localization of Bub1 and a Mad3/Bub1-related protein kinase. *J Cell Biol* 142(1):1–11.
- Malureanu LA, et al. (2009) BubR1 N terminus acts as a soluble inhibitor of cyclin B degradation by APC/C(Cdc20) in interphase. *Dev Cell* 16(1):118–131.
- Elowe S, et al. (2010) Uncoupling of the spindle-checkpoint and chromosome-congression functions of BubR1. *J Cell Sci* 123(Pt 1):84–94.
- Lara-Gonzalez P, Scott MI, Diez M, Sen O, Taylor SS (2011) BubR1 blocks substrate recruitment to the APC/C in a KEN-box-dependent manner. *J Cell Sci* 124(Pt 24):4332–4345.
- Tang Z, Bharadwaj R, Li B, Yu H (2001) Mad2-independent inhibition of APC/Cdc20 by the mitotic checkpoint protein BubR1. *Dev Cell* 1(2):227–237.
- Kallio M, Weinstein J, Daum JR, Burke DJ, Gorskys GJ (1998) Mammalian p55CDC mediates association of the spindle checkpoint protein Mad2 with the cyclosome/anaphase-promoting complex, and is involved in regulating anaphase onset and late mitotic events. *J Cell Biol* 141(6):1393–1406.
- Musacchio A, Salmon ED (2007) The spindle-assembly checkpoint in space and time. *Nat Rev Mol Cell Biol* 8(5):379–393.
- Guo Y, Kim C, Ahmad S, Zhang J, Mao Y (2012) CENP-E-dependent BubR1 autophosphorylation enhances chromosome alignment and the mitotic checkpoint. *J Cell Biol* 198(2):205–217.
- Suijkerbuijk SJ, et al. (2012) The vertebrate mitotic checkpoint protein BUBR1 is an unusual pseudokinase. *Dev Cell* 22(6):1321–1329.
- Li D, Morley G, Whitaker M, Huang JY (2010) Recruitment of Cdc20 to the kinetochore requires BubR1 but not Mad2 in *Drosophila melanogaster*. *Mol Cell Biol* 30(13):3384–3395.
- Conde C, et al. (2013) *Drosophila* Polo regulates the spindle assembly checkpoint through Mps1-dependent BubR1 phosphorylation. *EMBO J* 32(12):1761–1777.
- Hauf S (2013) The spindle assembly checkpoint: Progress and persistent puzzles. *Biochem Soc Trans* 41(6):1755–1760.
- D'Arcy S, Davies OR, Blundell TL, Bolanos-Garcia VM (2010) Defining the molecular basis of BubR1 kinetochore interactions and APC/C-CDC20 inhibition. *J Biol Chem* 285(19):14764–14776.
- Suijkerbuijk SJ, Vleugel M, Teixeira A, Kops GJ (2012) Integration of kinase and phosphatase activities by BUBR1 ensures formation of stable kinetochore-microtubule attachments. *Dev Cell* 23(4):745–755.
- Kruse T, et al. (2013) Direct binding between BubR1 and B56-PP2A phosphatase complexes regulate mitotic progression. *J Cell Sci* 126(Pt 5):1086–1092.
- Xu P, Raetz EA, Kitagawa M, Virshup DM, Lee SH (2013) BUBR1 recruits PP2A via the B56 family of targeting subunits to promote chromosome congression. *Biol Open* 2(5):479–486.
- Herzog F, Peters JM (2005) Large-scale purification of the vertebrate anaphase-promoting complex/cyclosome. *Methods Enzymol* 398:175–195.
- Gassmann R, et al. (2010) Removal of Spindly from microtubule-attached kinetochores controls spindle checkpoint silencing in human cells. *Genes Dev* 24(9):957–971.
- Holland AJ, Lan W, Niessen S, Hoover H, Cleveland DW (2010) Polo-like kinase 4 kinase activity limits centrosome overduplication by autoregulating its own stability. *J Cell Biol* 188(2):191–198.
- Tighe A, Johnson VL, Taylor SS (2004) Truncating APC mutations have dominant effects on proliferation, spindle checkpoint control, survival and chromosome stability. *J Cell Sci* 117(Pt 26):6339–6353.
- Meraldi P, Draviam VM, Sorger PK (2004) Timing and checkpoints in the regulation of mitotic progression. *Dev Cell* 7(1):45–60.
- Tang Z, Yu H (2004) Functional analysis of the spindle-checkpoint proteins using an in vitro ubiquitination assay. *Methods Mol Biol* 281:227–242.